Asian Research Journal of Mathematics

18(8): 35-47, 2022; Article no.ARJOM.88596
ISSN: 2456-477X

Magnetohydrodynamic Jeffrey Nanofluid Flow Over a Vertical Sheet

Wekesa Waswa Simon [a*] and Winifred Nduku Mutuku [a]

[a] Department of Mathematics and Actuarial Science, Kenyatta University, P.O. Box 43844-00100, Nairobi, Kenya.

Authors' contributions

This work was carried out in collaboration between both authors. Author WW Simon designed the study, performed the numerical analysis, wrote the protocol, the literature review and first draft of the manuscript. Author WNM managed, advised and guided the entire study. Both authors read and approved the final manuscript.

Article Information

DOI: 10.9734/ARJOM/2022/v18i830396

Open Peer Review History:
This journal follows the Advanced Open Peer Review policy. Identity of the Reviewers, Editor(s) and additional Reviewers, peer review comments, different versions of the manuscript, comments of the editors, etc are available here: https://www.sdiarticle5.com/review-history/88596

Original Research Article

Received 09 April 2022
Accepted 18 June 2022
Published 23 June 2022

Abstract

Aim: This study focuses on the numerical analysis of Jeffrey nano-fluid bound with magnetic field in presence of convectively heated boundary.
Study Design: Abstract, introduction, Equations formulation, numerical analysis and conclusion
Place and Duration of Study: Department of Mathematics and Actuarial Science, Kenyatta University, between 2021-2022
Methodology: This paper discusses the imposed magnetic field on Jeffrey fluid suspended with nanometre-sized particles moving over a vertical sheet with a convectively heated boundary. The partial differential equations are formulated by considering assumptions and the boundary conditions to describe the continuity, momentum, energy and concentration of the fluid. The similarity transformation technique was applied to convert the partial differential equations into first-order linear differential equations which were simulated in Matlab by invoking the Adam's-Moulton predictor-corrector scheme in ode113.
The graphs have been analysed with the effects of Deborah, Dufour-Lewis, Hartman, and Prandtl numbers respectively, solutal stratification, diffusion, thermophoresis, temperature Grashof, mass Grashof, relaxation-retardation parameters on the flow velocity, concentration, temperature, skin friction, heat and mass transfers looked into.
Results: While Deborah number increased velocity, it reduced concentration, skin friction and thermal

**Corresponding author: Email: swekesa16@gmail.com;*

boundary layer at lower numbers hence improved mass and heat transfer. Solutal stratification, Retardation-relaxation parameter and diffusion raised temperature thus heat transfer.
Conclusion: Deborah number, solutal stratification, retardation-relaxation parameter and diffusion improves heat and mass transfer.

Keywords: Base fluid; nanofluid; magneto-hydrodynamic; brownian diffusion; thermophoresis.

1 Introduction

Nanofluid is a uniform suspension of nanometre-sized metal particles in a base fluid. Metal microparticles of a diameter between 1-100nm are commonly used. Nanoparticles can be obtained from metals, oxides, carbon, nanotube and carbides. Base fluids include water, ethylene, oil, glycol, paraffine and ethanol while metals include Copper, aluminium, gold, and mercury. Nanofluid has better heat conductivity than the base fluid. Nanofluids are used to eject heat from nuclear reactors, cancer therapeutics, sensory and imaging, in nano dry delivery, as coolants in electronic components, nuclear reactors, heat exchangers and in solar generation systems due to the enhanced thermal conductivity properties of nanofluids for heat transfer. The concentration, size and material of the nanoparticle determine thermal conductivity.

Zokri SM, et al. [1] studied the flow and heat transfer of magnetohydrodynamic Jeffrey nanofluid induced by a passively moving plate and numerically examined it. The findings, physical parameters over temperature profiles, Using the Runge Kutta Fehlberg method agreed with the previous model.

Ijaz M, et al. [2] Discussed the mixed convective flow of Jeffrey fluid near the axisymmetric stagnation point over an inclined permeable stretching cylinder where the results showed that temperature is a decreasing function of the thermal stratification parameter.

Murtaza S, et al. [3] Analyzed the nonlinear fractionalized Jeffrey fluid with the novel approach of the Atangana Bleanu fractional model where the results showed that the fractional model provided more than a line as compared to the classical model.

Ur Rasheed H, et al. [4] Studied attributes of the convective flow of Jeffrey nanofluid with a vertical stretching plane surface incorporating magnetic influence. Among other results, it was shown that velocity profile diminished with large Hartman numbers.

Agbaje TM et al. [5] Researched natural convection viscoelastic Jeffrey's nanofluid flow from a vertical permeable flat plate with heat generation, thermal radiation and chemical reaction. The findings depicted that Debora number and suction parameter had related effects on the velocity profile.

El-Zahar ER, et al. [6] Examined the influence of viscous dissipation and Brownian motion on Jeffrey nanofluid over an unsteady moving surface with thermophoresis and mixed convection where graphical outcomes indicated that augmentation buoyance ratio and thermophoresis parameter led to diminished velocity curves and increased temperature curve.

Ur Rasheed H, et al. [7] Researched effects of Joule heating and viscous dissipation on magnetohydrodynamic boundary layer flow of Jeffrey fluid over a vertically stretching cylinder. A larger Schmidt number decreased the concentration profile while it increased with a larger thermophoresis parameter.

Ge-JiLe H, et al.[8] Explored slip flow of Jeffrey nanofluid with activation energy and entropy generation application. The findings were that slipped phenomena decay velocity profile while temperature and concentration directly related with Brownian motion parameter and activation energy.

According to Ge-JiLe H, et al. [9], in the research on the Atangana Baleanu fractional model for the flow of Jeffrey nanofluid with diffusion thermo-effects applied in engine oil, the efficiency of engine oil improved when silver nanoparticles were increased.

Srinivasacharya D [10] on mixed convection flow of a nanofluid in a vertical channel with a hall and ion slip effect observed that velocity increased at the hot wall and decreased at the cold wall due to increasing Jeffrey parameter.

Hayat T [11] Enquired mechanism of the nonlinear convective flow of Jeffrey nanofluid due to nonlinear radially stretching sheet with convective conditions and magnetic field and found out that Deborah number enhanced velocity profile while thermal radiation enhanced temperature and heat transfer.

Shahzad F [12] Discussed numerical simulation of magnetohydrodynamic Jeffrey nanofluid and heat transfer over a stretching sheet considering Joule heating and viscous dissipation and concluded that silver water nanofluids have less velocity, local Nusselt number and local skin frictions than those of the base fluid. An increase in Deborah's number increased skin friction and Nusselt number which decreased by increased magnetic parameter.

Saleem S [13] In the enquiry of magneto Jeffrey nanofluid biconvection over a rotating vertical cone due to gyrotactic microorganisms observed that biconvection Rayleigh number and Schmidt number shrank the magnitude of tangential velocity and augmented the reduced density of the motile microorganisms respectively.

Rasool G [14] In the investigation of Darcy Forchheimer's relation in magnetohydrodynamic Jeffrey nanofluid flow over a stretching surface noted that inertia and porosity factors declined momentum boundary while it increased the concentration of nanoparticles. From the foregoing none has posted about magnetohydrodynamic Jeffrey nanofluid flow over a vertical sheet which this work discusses to establish its suit for effective heat transfer.

2 Mathematical Formulation

Navier-stokes equation does not describe all the rheological properties of the fluids used in technology and industries. The preferred non-Newtonian fluids are classified as differential and rate types. The rate type has relaxation and retardation time. Jeffrey fluid is one of the rate types possessing linear viscoelastic feature which is applied in the manufacture of polymers. [12] stated that the steady time-independent derivative model $\tau = -PI + \frac{\mu}{1+\lambda_1}\left[R_1 + \lambda_2\left(\frac{\partial R_1}{\partial t} + \nabla v\right)R_1\right]$ where P is the pressure, τ the Cauchy stress tensor, R_1 Rivlin-Ericksen tensor stated as $R_1 = \nabla v + \nabla v^t$. If $\lambda_1 = \lambda_2$, this model reduces to Navier-stokes equation; the fluid becomes Newtonian. Retardation time explains the Jeffrey temperature flux model while relaxation time describes the time of fluid restoration from the deformed position to the initial stable state. Assuming that two-dimensional flow is streamlined, incompressible and an electrically conducting Jeffery nanofluid over a vertical sheet with plate y=0 and the fluid is magneto-hydrodynamically time-independent. The x-axis is perpendicular to the vertical sheet.

2.1 Equations Governing the Fluid Flow

[8] used Buongiorno model with Brownian diffusion and thermophoresis in absence of turbulent effect\external forces to derive the conservative equations. The formulation of continuity, momentum, energy and concentration equations have regulated the aforementioned model.

$$\frac{\partial u}{\partial x} + \frac{\partial v}{\partial y} = 0 \qquad 2.1.0$$

$$u\frac{\partial u}{\partial x} + v\frac{\partial u}{\partial y} = \beta g(T - T_\infty) + g\beta^*(C - C_\infty) + \frac{\gamma}{1+\lambda_1}\left(\frac{\partial^2 u}{\partial y^2} + \lambda_2\left(u\frac{\partial^3 u}{\partial x \partial y^2} + \frac{\partial u}{\partial y}\frac{\partial^2 u}{\partial x \partial y} - \frac{\partial u}{\partial x}\frac{\partial^2 u}{\partial y^2} + v\frac{\partial^3 u}{\partial y^3}\right)\right) - \frac{\sigma B_0^2 u}{\rho} \qquad 2.1.1$$

$$u\frac{\partial T}{\partial x} + v\frac{\partial T}{\partial y} = \alpha\frac{\partial^2 T}{\partial y^2} + \frac{\sigma B_0^2 u^2}{\rho c_p} + \tau\left[D_B\frac{\partial T}{\partial y}\frac{\partial C}{\partial y} + \frac{D_f}{T_\infty}\left(\frac{\partial u}{\partial y}\right)^2\right] \qquad 2.1.2$$

$$u\frac{\partial C}{\partial x} + v\frac{\partial C}{\partial y} = D_B\frac{\partial^2 C}{\partial y^2} + \frac{D_T}{T_\infty}\frac{\partial^2 T}{\partial y^2} \qquad 2.1.3$$

Subject to the boundary conditions at the surface of the vertical sheet and the free streams of the above equations expressed as

$$\left.\begin{array}{c} u=0, v=0, T=T_{\omega}(x), -k_{\omega}\frac{\partial T}{\partial y}=h_{\omega}(T_{\omega}-T), C=C_{w}(x)\ at\ y=0 \\ u\to 0, v\to 0, T\to T_{\infty}(x), C\to C_{\infty}(x),\ as\ y\to\infty \end{array}\right\} \quad 2.1.4$$

where u and v are the velocity components along the x-axis and y-axes direction respectively, $\gamma=\frac{\mu}{\rho}$ is the kinematic viscosity, λ_1 the ratio of relaxation time, λ_2 retarding time, β is the thermal expansion coefficient of the fluid, ρ is the fluid density, g is the acceleration due to gravity, β^* is the volumetric expansion coefficient of the fluid, T_w is the boundary temperature of the fluid, C_w is the particle volume fraction on the boundary of the magnetic field, D_B is the Brownian diffusion coefficient, U_∞ is the free stream velocity on the boundary, T_∞ temperature of the particle far away from the fluid, C_∞ is the particle volume fraction far away from the fluid, and B is the imposed magnetic field, D_T is the thermophoretic diffusion coefficient, C_p is specific heat at constant pressure, τ is the ratio of heat capacity, σ is the electrical conductivity and ∞ is the value far away from the surface.

2.2 Transformation of the nonlinear equations

The set of equations describing this flow is non-linear. To solve them, they were transformed into a set of ordinary differential equations by the similarity transformation method.

2.2.1 Similarity transformation

By introducing the similarity transformation variables

$$\eta=\left(\frac{a}{v}\right)^{\frac{1}{2}}y, \psi=(av)^{\frac{1}{2}}xf$$

the boundary conditions and the partial differential equations 2.1.0-2.1.4 are transformed to

$$u=u_w=ax, v=0, T=T_w, C=C_w\ at\ y=0$$

$$u=0, T\to T_\infty, C\to C_\infty \quad as\ y\to\infty$$

The free stream and the stream functions variables in this work are related to velocity along the x and y axes respectively as

$$u=\frac{\partial\psi}{\partial y} \text{ and } v=-\frac{\partial\psi}{\partial x} \quad 2.2.1.1$$

Substituting Eqn.2.2.1.1 into equation 2.1.0

$$\frac{\partial}{\partial x}\left(\frac{\partial\psi}{\partial y}\right)+\frac{\partial}{\partial y}\left(-\frac{\partial\psi}{\partial x}\right)=0$$

Partially differentiating the introduced similarity transformation variables and substituting the result into equations 2.2.1.1,2.1.1-2.1.3 yield

$$u=axf', v=-(av)^{1/2}f$$

$$f'''-(1+\beta_1)((f')^2-ff''+Ha^2f'-Gr-Gr^*)-\beta_2((f'')^2+f^{iv})=0 \quad 2.2.1.2$$

$$\theta f'+f'\alpha-\theta' f-Ha^2Ec(f')^2-\theta'\phi' N_b-N_t(\theta'')^2-\frac{\theta''}{Pr}=0 \quad 2.2.1.3$$

$$\phi f'+f'-f\phi'-Ld\theta'\phi-\frac{\phi''}{Ln}=0 \quad 2.2.1.4$$

bearing upon the boundary conditions

$$\left.\begin{array}{c} f=0, f^{'}=1, \theta^{'}=-Bi(1-\theta), \phi=1 \; at \; \eta=0 \\ f^{'}=0, \theta=0, \phi=0 \; at \; \eta=\infty \end{array}\right\} \qquad 2.2.1.5$$

Where

$$N_t=\frac{\tau D_T b^2 x}{\nu T_\infty} \; , \alpha=\frac{n}{m}, N_b=\frac{\tau D_B m x}{\nu} \; , Ec=\frac{a^2 x}{C_p} \; , \phi=\frac{C_w-C_\infty}{C_\infty}$$
$$Ha^2=\frac{\sigma B_0^2}{\rho a}, Ld=\frac{D_T(T_\omega-T_\infty)bx}{\nu T_\infty}, Ln=\frac{\nu}{D_B} \; , G_r=\frac{g\beta(b-c)}{a^2}, G_r^*=\frac{g\beta^*(m-n)}{a^2}$$
$$\beta_2=\lambda_2 a \; , Pr=\frac{\alpha}{\nu}, \beta_1=(1+\lambda_1)$$

are thermophoresis, solutal stratification and diffusion parameters, Eckert, Hartman, DuFour Lewis, Nano-Lewis, Temperature Grashof, mass Grashof, Deborah and Prandtl numbers respectively, β_1, a Jeffrey fluid parameter, θ temperature, ϕ concentration and f dimensionless stream function, η similarity variable and ψ the stream function.

The skin friction coefficient Cf_x , Heat transfer rate (Nusselt number) Nu_x and mass transfer rate (Local nano-Sherwood number) Sh_x prescribed as

$$Cf_x=\frac{\tau_\omega}{\rho(u_\omega^2)} \; , Nu_x=\frac{q_\omega}{k(T_\omega-T_\infty)} \; , Sh_x=\frac{q_m}{D_B(C_\omega-C_\infty)}$$

With the surface nano-shear stress τ_ω, surface nano heat flux q_ω and surface nano mass flux q_m expressed as

$$\tau_\omega=\mu\frac{\partial u}{\partial y} \; , q_\omega=-k\frac{\partial T}{\partial y} \; , q_m=D_B\frac{\partial C}{\partial y}$$

By appropriate substitution, the skin friction coefficient, Nusselt number and Sherwood numbers obtained are $Cf_x Re_x^{\frac{1}{2}}=f^{''}, Nu_x Re_x^{-\frac{1}{2}}=-\theta^{'}, Sh_x Re_x^{-\frac{1}{2}}=\phi^{'}$ with $Re_x=\frac{xa}{\nu}$ as the Local Reynolds number.

3 Numerical Procedure

The linear-less boundary equations 2.2.1.2-2.2.1.4 subject to the boundary condition 2.2.1.5 are solved numerically using the Adams-Moulton predictor-corrector scheme by first converting to states variable form and invoking Matlab bvp5c function.

3.1 States variable form

$$x_1=f, x_2=f^{'}, x_3=f^{''}, x_4=f^{'''}, x_5=f^{iv}, x_6=\theta, x_7=\theta', x_8=\theta^{''}, x_9=\phi, x_{10}=\phi^{'},$$
$$x_{11}=\phi^{''}$$
$$x_1^{'}=x_2$$
$$x_2^{'}=x_3$$
$$x_3^{'}=x_4$$
$$x_4^{'}=(1+\beta_1)(x_2^2-x_1x_3+Ha^2x_2-Gr-Gr*)-\beta_2(x_3^2+x_5)$$
$$y_5^{'}=x_6$$
$$x_6^{'}=x_7$$
$$x_7^{'}=Pr[x_2x_6+x_1\alpha-xx_7+HaEcx_2^2-x_7x_{10}N_b-x_8^2N_t]$$
$$x_8^{'}=x_9$$
$$x_9^{'}=x_{10}$$
$$x_{10}^{'}=Ln(x_9x_2+x_2-x_1x_{10}-x_7x_{10}Ld)$$

Subject to the dimensionless boundary conditions

$$x_1 = 0, x_2 = 1, x_7 = -Bi(1 - x_6), x_9 = 1 \; at \; \eta = 0$$
$$x_2 = 0, x_6 = 0, x_9 = 0 \; at \; \eta = \infty$$

Graphical Analysis:

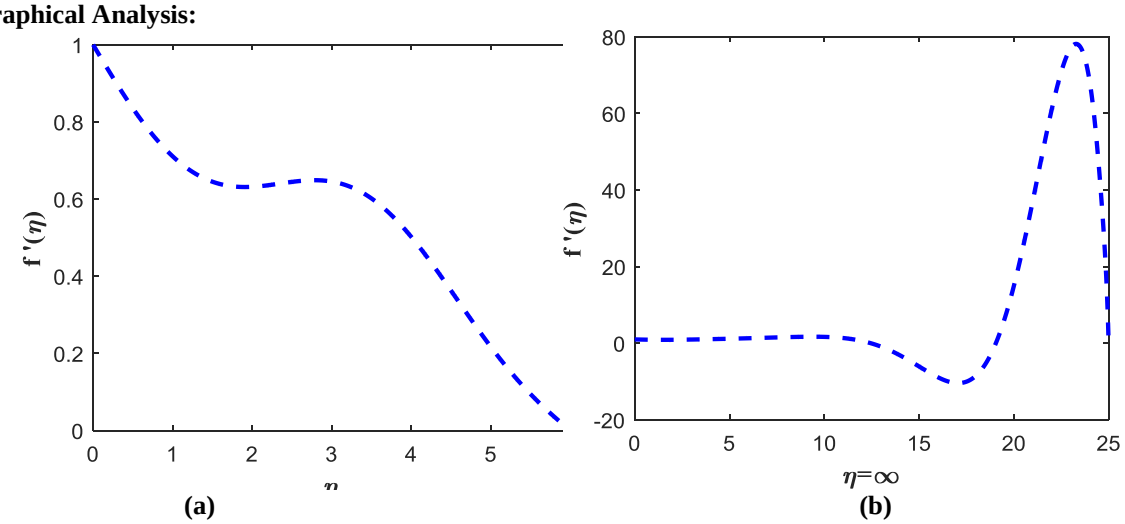

Fig. 1. (a) and (b) Boundary conditions

This study looks into the effects of Hartman, Deborah, Prandtl, Mass Grashof, temperature Grashof, solutal stratification, relaxation-retardation, thermophoresis, diffusion, Dufour on velocity, temperature, concentration and the consequences to skin friction, Nusselt and Sherwood numbers in presence of convectively heated boundary from Fig. 1 to Fig. 31.

The graphs in Fig.1. (a) and (b) satisfy the boundary conditions of equation 2.1.4

Velocity profiles:

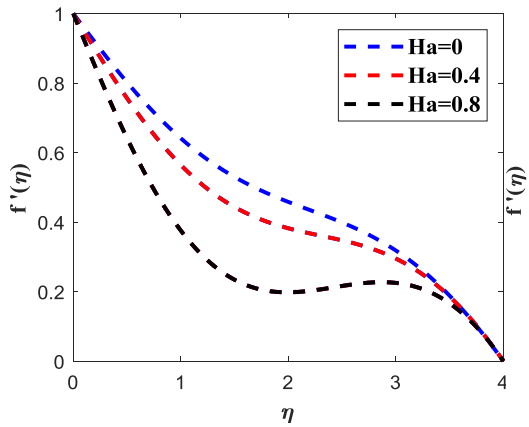

Fig. 2. Effect of Hartman number

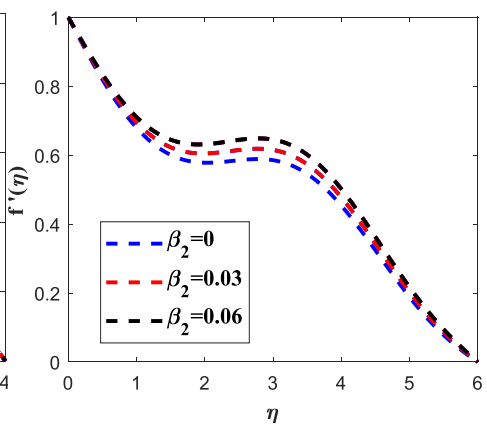

Fig. 3. Effect of Deborah's number

Pr=6.1,Ld=0.3,B=1 , β_1 =0.1, , β_2 =0.06,Gr=0.3, Pr=6.1,Ld=0.3,B=1, β_1 =0.1,Gr=0.3,Gr*=0.3, Gr*=0.3,N_b=1.3,N_t=1.2,L=1.5,Ec=0.1,α=0.2 N_b=1.3,N_t=1.2,L=1.5,Ha=0.1,E=0.1, α =0.2

Figs. 2,4,8 and 7 depict an increase in Hartman number, Prandtl number, Relaxation-Retardation and solutal stratification together with the similarity variable decreased velocity. The magnetic field interacts with the electrically conducting Jeffrey nanofluid to cause a Lorenz force which slows down velocity. The increase in Prandtl number increases thermal diffusivity and thermal boundary layer. This is due to the increased rate of Jeffrey nanoparticle fluid collisions, reduced buoyant force, heat dissipation and viscosity. The density of the nanofluid determines stratification. The layering has a similar effect. From figs. 3,5,6 to 9 show that an increase

in Deborah number, Mass Grashof, thermophoresis and mass temperatures lead to a corresponding increase in velocity; decreased resistance in the boundary layer caused by higher buoyant forces, temperature and migration of fresh mass particles.

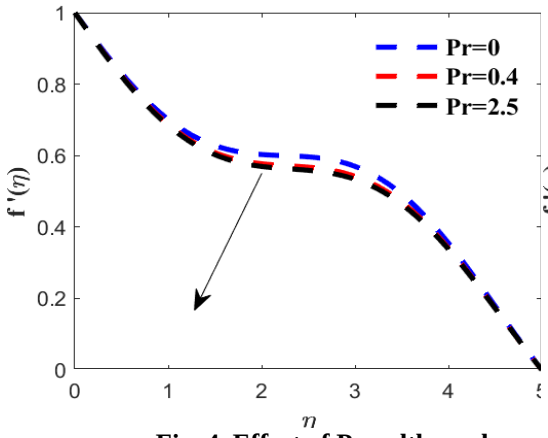

Fig. 4. Effect of Prandtl number

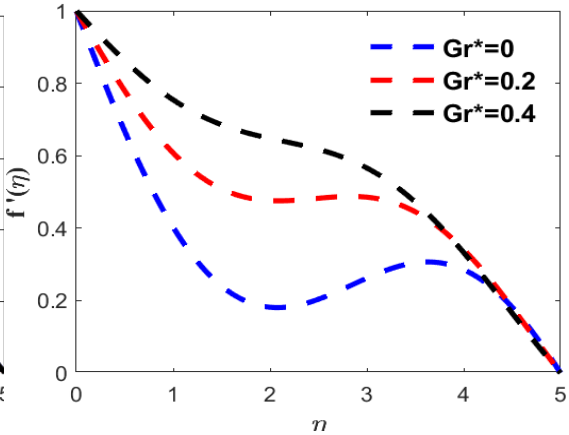

Fig.5. Effect of mass Grashof

Ld=0.3,B=1, β_1 =0.1, β_2 =0.06,Gr=0.3, Pr=2.5,Ld=0.3,B=1, β_1 =0.1, β_2 =0.06,Gr=0.3, Gr*=0.3,N_b=1.3,N_t=1.2,L=1.5,Ha=0.1,Ec=0.1, α =0.2, N_b=1.3,N_t=1.2,L=1.5,Ha=0.1,Ec=0.1, α =0.2

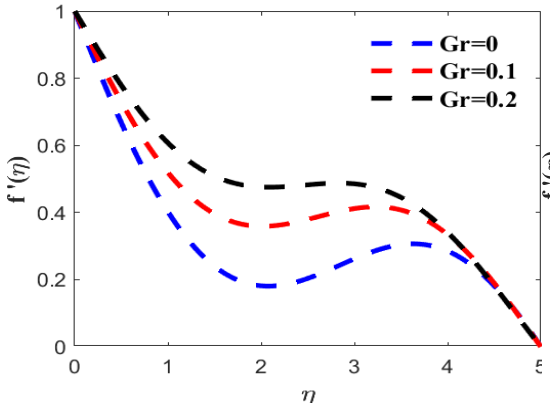

Fig. 6. Effect of mass temperature

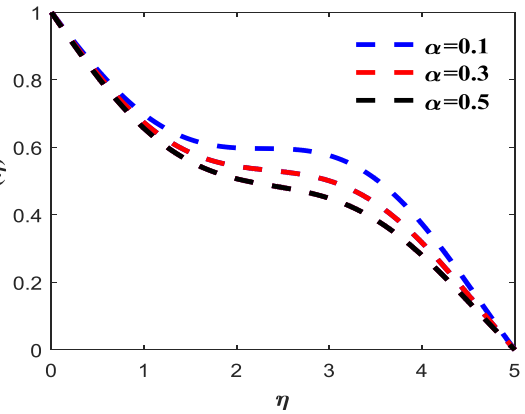

Fig. 7. Effect of solutal stratification

Pr=2.5,Ld=0.3,B=1, β_1 =0.1, β_2 =0.06,Gr* =0.3, Pr=6.2,Ld=2.4,B=1, β_1 =0.1, β_2 =0.06, N_b=1.3,N_t=1.2,L=1.5,Ha=0.1,Ec=0.1, α =0.2, Gr=0.3,Gr*=0.3,N_b=1.3,N_t=1.2,L=1.5,Ha=0.1,Ec=0.1

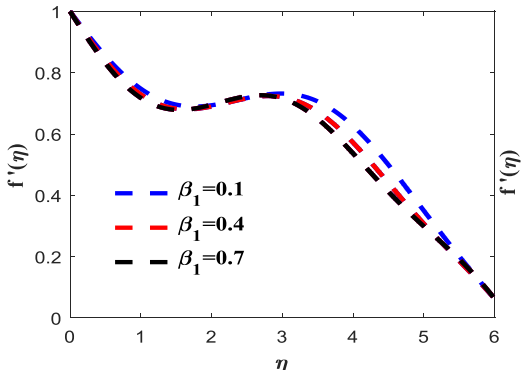

Fig. 8. Effect of relaxation-retardation

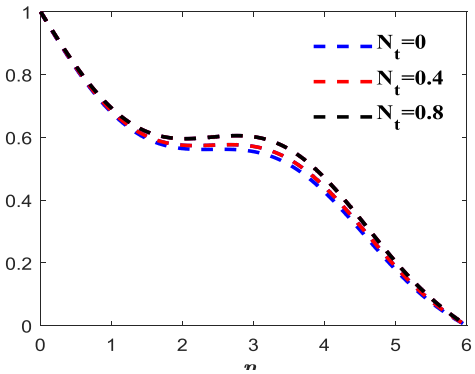

Fig. 9. Effect of thermophoresis

Pr=6.2, Ld.=2.4, B=1, β_2 =0.06, Gr=0.3, Gr*=0.3, Pr.=6.2, Ld.=2.4, B=1, β_1 =0.1, β_2 =0.06, Gr=0.3,Gr*=0.3, N_b=1.3,N_t=1.2,L=1.5,Ha=0.1,Ec=0.1, α = 0., N_b=1.3,L=1.5,Ha=0.1,E=0.1, α = 0.2

Temperature profiles:

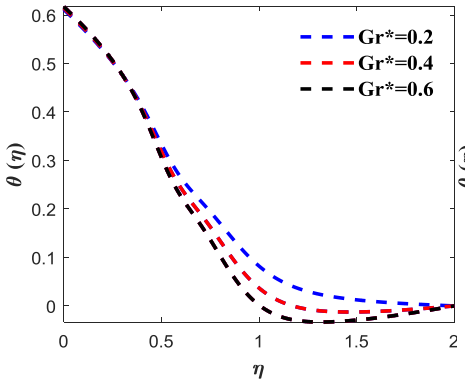

Fig. 10.Effect of mass Grashof

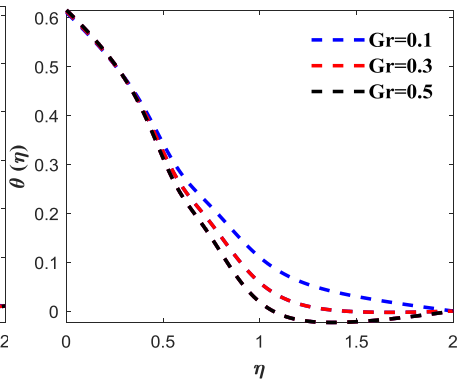

Fig. 11. Effect of temperature Grashof

Pr=6.2, Ld=2.4, B=1, β_1 =0.1, β_2 =0.06, Gr=0.3, Pr=6.2, Ld=2.4, B=1, β_1 = 0.1 β_2 =0.06,Gr*=0.3, N_b=1.3,N_t=1.2,L=1.5,Ha=0.1,Ec=0.1, α = 0.2, N_b=1.3,N_t=1.2,L=1.5,Ha=0.1,Ec=0.1, α = 0.2

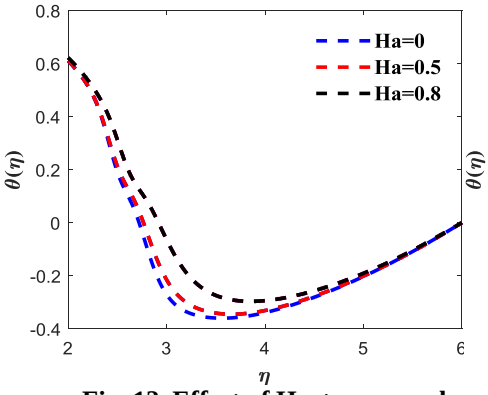

Fig. 12. Effect of Hartman number

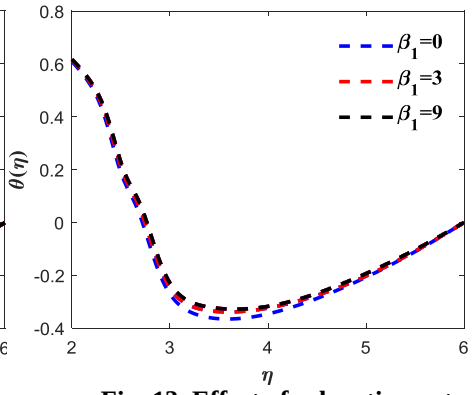

Fig. 13. Effect of relaxation-retardation

Pr=6.2, Ld=2.4, B=1, β_1 = 0.1, β_2 =0.06,Gr*=0.3, Pr=6.2, Ld=2.4, B=1,β_2 =0.06, Gr=0.3, N_b=1.3,N_t=1.2,L=1.5,Ec=0.1, α = 0.2, Gr*=0.3,N_b=1.3,L=1.5,Ha=0.1,Ec=0.1, α = 0.2

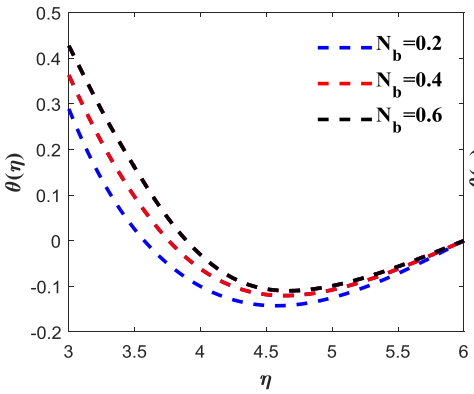

Fig. 14. Effect of Diffusion

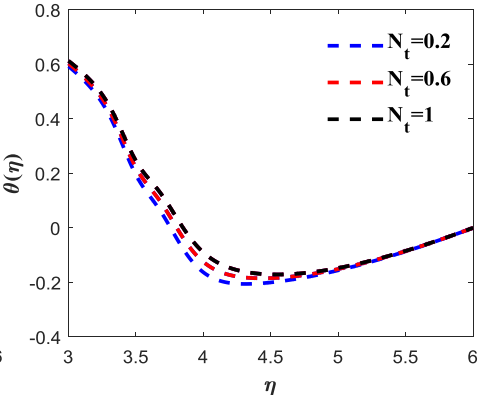

Fig. 15. Effect of thermophoresis

Pr=6.2, Ld=2.4, B=1, β_1 =0.3, β_2 =0.06, Gr=0.3, Pr=6.2, Ld=2.4, B=1, β_1 =0.3, β_2 =0.06, Gr=0.3, Gr*=0.3,N_t=1.2,L=1.5,Ha=0.1,Ec=0.1, α =0.2, Gr*=0.3,N_b=1.3,L=1.5,Ha=0.1,Ec=0.1, α =0.2

Figs. 10 and 11 show that an increase in mass and temperature Grashof decrease temperature as a result of reduced viscosity and collision rate between the influx of fresh and heated particles. Figs.12-15 infer the growth of Hartman number, retardation-relaxation, diffusion and thermophoresis increase temperature. The viscosity of

nano-particles and the resistive of the electromagnetic field hike temperature. Nano-particles distribute energy from convectively heated boundaries to other particles at a lower temperature.

Concentration profiles:

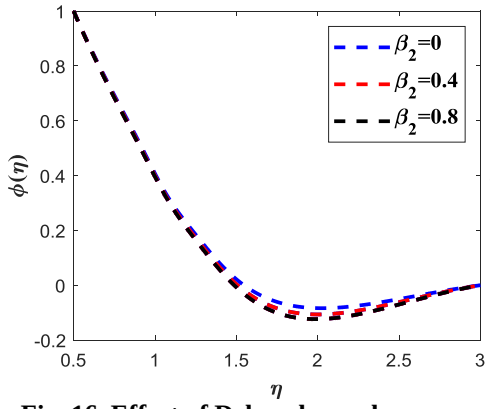

Fig. 16. Effect of Deborah number

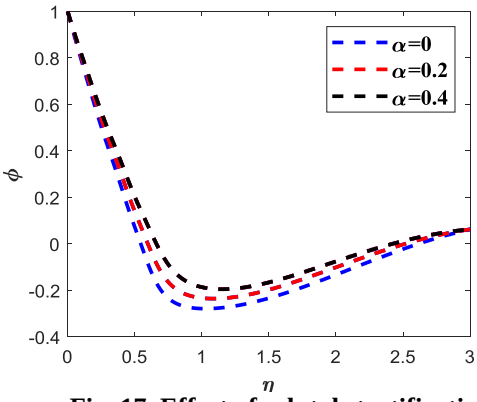

Fig. 17. Effect of solutal stratification

Pr=6.2, Ld=2.4, B=1, β_1 =0.3,Gr=0.3,Gr*=0.3,N_b=1.3, Pr=6.2, Ld=2.4, B=1, β_1 =0.3 , β_2=0.4,Gr=0.3,Gr*=0.3, N_t=1.2,L=1.5,Ha=0.1,Ec=0.1, α =0.2, N_b=1.3,L=1.5,Ha=0.1,Ec=0.1, α =0.2

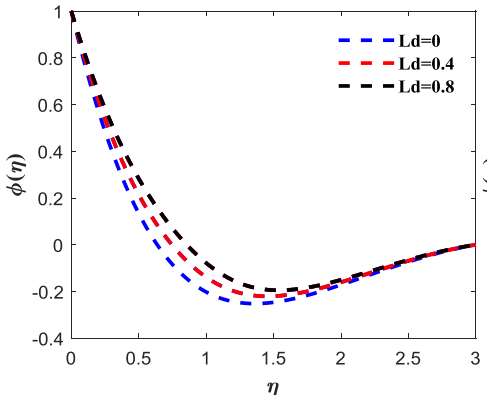

Fig. 18. Effect of Dufour number

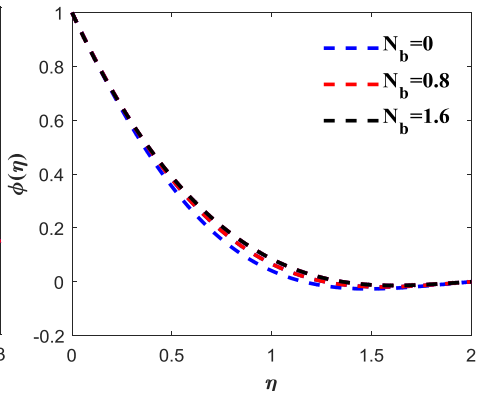

Fig. 19.Effect of Diffusion

Pr=6.2, B=1, β_1 =0.3, β_2 =0.4, Gr=0.3,G=0.3,N_b=1.3, Pr=2,Ld=1.6,B=1, β_1 =0.3, β_2 =0.4,Gr=0.3,G=0.3, L=1.5,Ha=0.1,Ec=0.1, α =0.2,N_t=1.2, N_b=1.6,N_t=1.2,L=1.5,Ha=0.1,Ec=0.1, α =0.2

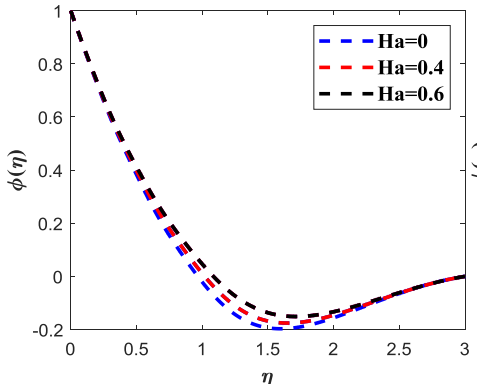

Fig. 20. Effect of Hartman number

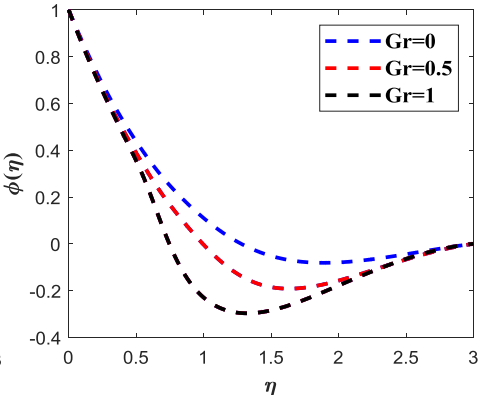

Fig. 21. Effect of temperature Grashof

Pr=6.2,Ld=2.4,B=1, β_1 =0.3 , β_2 =0.4,Gr=0.3,Gr*=0.3, Pr=2,Ld=2.4,B=1, β_1 =0.3 , β_2 =0.4,Ha=0.1,G=0.3,L=1.5, L=1.5,Nb=0.8,Ha=0.1,Ec=0.1, α =0.2,N_t=1.2 , N_b=0.8,N_t=1.2,Ha=0.1,Ec=0.1, α =0.2

From figs. 16 and 21, Deborah number and temperature Grashof thins concentration.

Skin friction and Nusselt number:

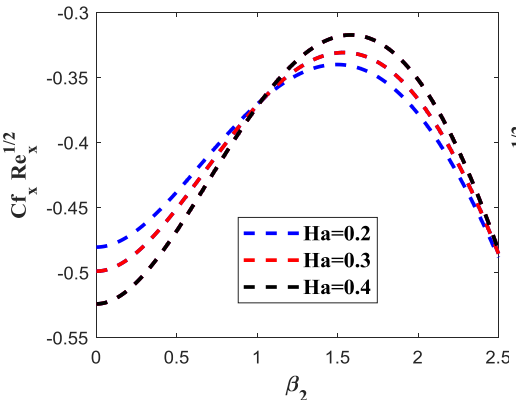

Fig. 22. Effects of Hartman and Deborah numbers

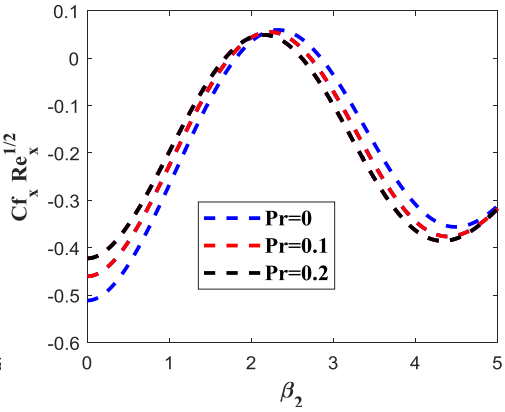

Fig. 23. Effects of Prandtl and Deborah numbers

Pr=6.2, Ld=2.4, B=1, β_1 =0.3, β_2 = 0.8, Gr=0.3,Gr*=0.3,N_b=1.6,N_t=1.2, Ld=2.4, B=1, β_1 =0.3, β_2 = 0.8,Gr=0.3,Gr*=0.3, L=1.5,Ec=2.5, α =0.2, N_b=1.6,N_t=1.2,L=1.5,Ec=2.5,Ha=0.4, α =0.2

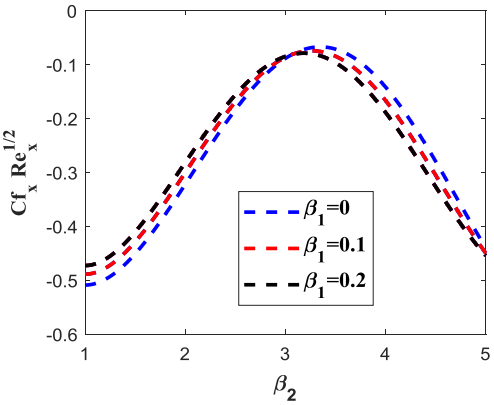

Fig. 24. Effects of retardation-relaxation and Deborah

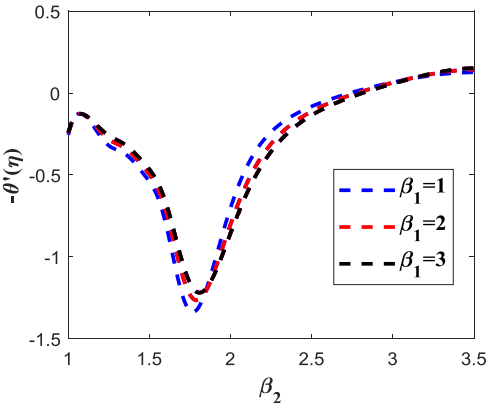

Fig. 25. Effects of Retardation-relaxation and Deborah

Ld=2.4, B=1,Pr=0.4,Gr=0.3,Gr*=0.3,N_b=1.6,N_t=1.2, Ld=2.4, B=1,Pr=0.4,Gr=0.3,G=0.3,N_b=1.6,N_t=1.2, L=1.5,Ec=2.5,Ha=0.4, α =0.2, L=1.5,E=2.5,Ha=0.4, α =0.2

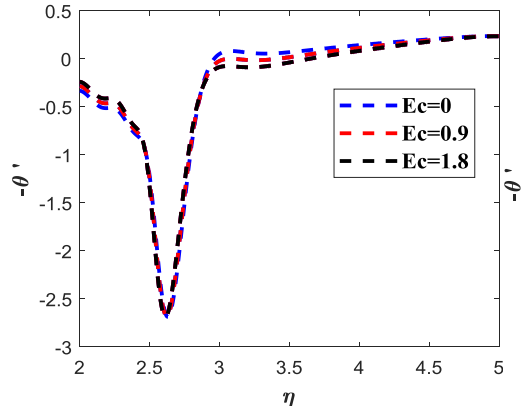

Fig. 26. Effect of Eckert number

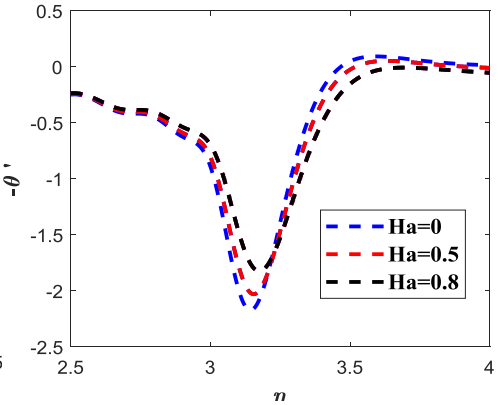

Fig. 27. Effect of Hartman number

Pr=6.2,Ld=2.4, B=1, β_2 =0.3, β_2 =0.8,Gr=1,Gr*=0.3, Pr=6.2,Ld=2.4, Bi=1 , β_1 =0.3, β_1 ==0.8,Ec=0.1 N_b=1.6,N_t=1.2,L=1.5,Ha=0.4, α =0.2, Gr=1,Gr*=0.3,N_b=1.6,N_t=1.2,L=1.5, α =0.2

Few nano-particles settle in the high resistive boundary while mass temperature increment lessens the density of nano-particles causing diffusion. Figs.17-20, it is clear that concentration improves with a gain of solutal stratification, DuFour number, diffusion and Hartman number. At constant density, nano-particles arrange according to size and heat absorbed. The layers pack increasing concentration. The increase in the Dufour number decreases the temperature between the boundary layer and the wall. The temperature gradient results in more heat transfer to the fluid. This lowers internal fluid friction. Similarly, thermophoresis dispenses nano-particles subject to changed density.

Fig. 22-24 portray the concurrent effects of increasing Deborah numbers, Hartman numbers, Prandtl number and relaxation-retardation parameter on skin friction. It is noted in fig.22. the skin friction thins at lower numbers of Deborah and Hartman while it thickens at higher numbers; the boundary strata velocity increases. The opposite is observed in fig.23 and 24.

Fig. 25, Deborah number and solutal stratification enhances thermal conductivity by nano-particle conduction at 1 and convection for values greater than 1 . Thermal boundary shrinks at lower numbers. The same effect is observed in figs. 26 and 27.

Sherwood Number:

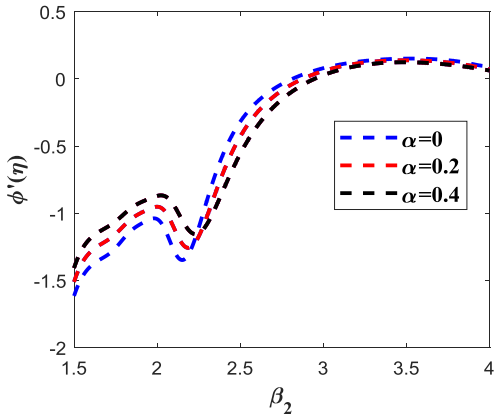

Fig. 28. Effects of solutal stratification and Deborah numbers

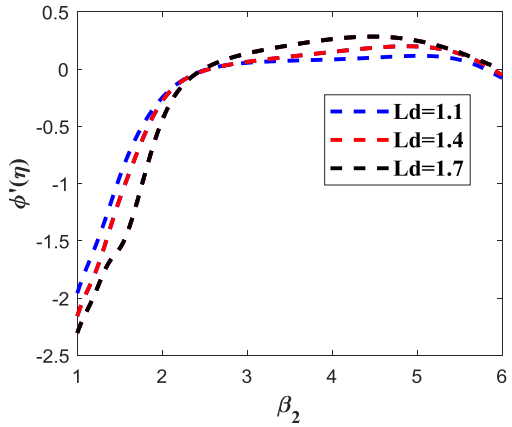

Fig. 29. Effect of Dufour-Lewis and Deborah numbers

Pr=6.2,Ld=2.4,B=1,Gr=0.3,Gr*=0.3,N_b=1.6,N_t=1.2, Pr=6.2, Ld=2.4, B=1, β_1=0.3, Gr=0.3, Gr*=0.3, N_b=1.6, L=1.5,Ha=0.1,Ec=2.5, α =0.2, N_t=1.2,,L=1.5, Ha=0.1,Ec=2.5, α=0.2

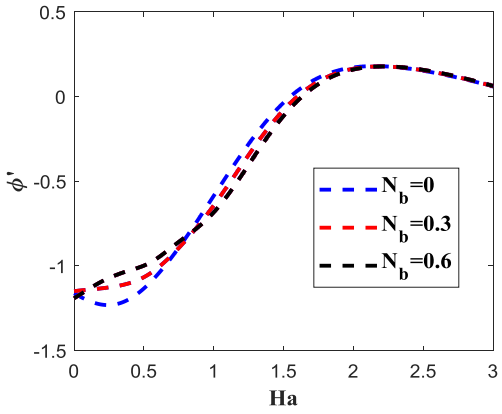

Fig. 30. Effects of Hartman number and diffusion

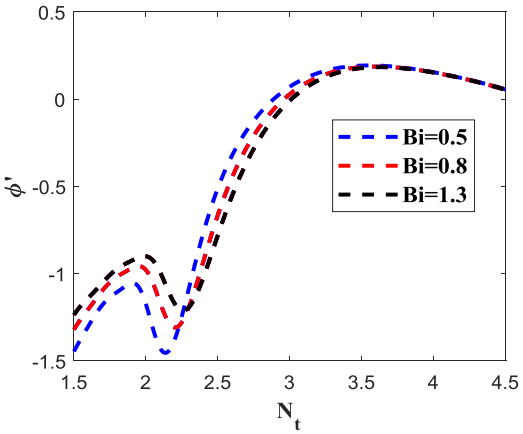

Fig. 31. Effects of thermophoresis & Biot number

Pr=6.2,Ld=2.4,B=1, 1 =0.3, β_2 =0.2,Gr=1,Gr*=0.3, Pr=6.2,Ld=2.4, β_1 =0.3, β_2 =0.2,Gr=1,Gr*=0.3, N_t=1.2,L=1.5,Ec=0.1, α=0.4, Nb=1.3,L=1.5,Ha=0.8,Ec=0.1, α=0.4,Ha=0.8, Nt=1.2

Figs. 28-29 illustrate the influence of Deborah number, DuFour -Lewis, Biot and Hartman numbers, thermophoresis, diffusion and solutal stratification. Figs.28,30 and 31 discover that a low number of the aforementioned parameters enhance mass transfer. The contrary is seen in Fig. 29.

4 Conclusion

While the increase in Hartman and Prandtl numbers, Relaxation-Retardation and solutal stratification decreased velocity, Deborah number, Mass Grashof, thermophoresis and mass temperatures increased it.

On the other hand growth in mass-temperature, Grashof lowered temperature, Hartman number, retardation-relaxation, diffusion and thermophoresis raised it.

Deborah number and temperature Grashof thinned concentration, solutal stratification, DuFour number, diffusion and Hartman number improved the concentration. Lower numbers of Deborah and Hartman shrank the skin friction. Large numbers thickened it. Solutal stratification and Deborah number widened the skin friction which increased heat transfer.

Deborah number and solutal stratification shrank thermal boundary at lower numbers. It is discovered that low numbers of Deborah, DuFour -Lewis, Biot and Hartman, thermophoresis, diffusion and solutal stratification enhance mass transfer. The opposite is evidenced by Dufour Lewis and Deborah's numbers.

Acknowledgement

I acknowledge the academic and research management of Dr. Winifred Nduku Mutuku for her expertise in fluid mechanics, numerical analysis, rigorous coaching, guidance and always being available for assistance.

Competing Interests

Authors have declared that no competing interests exist.

References

[1] Zokri SM, Arifin NS, Kasim AR, Mohammad NF, Salleh MZ. Boundary layer flow over a moving plate in MHD Jeffrey nanofluid: A revised model. InMATEC Web of Conferences 2018 (Vol. 189, p. 02005). EDP Sciences.
Available:https://doi.org/10.1051/matecconf/201818902005

[2] Ijaz M, Ayub M. Thermally stratified flow of Jeffrey fluid with homogeneous-heterogeneous reactions and non-Fourier heat flux model. Heliyon. 2019 Aug 1;5(8):e02303.
Available:https://doi.org/10.1016/j.heliyon.2019.e02303

[3] Murtaza S, Ali F, Aamina NA, Sheikh NA, Khan I, Nisar KS. Exact analysis of non-linear fractionalized Jeffrey fluid. A novel approach of Atangana–Baleanu fractional model. Computers, Materials & Continua. 2020 Jan 1;65(3):2033-47.
Available:https://doi.org/10.32604/cmc.2020.011817

[4] Ur Rasheed H, AL-Zubaidi A, Islam S, Saleem S, Khan Z, Khan W. Effects of Joule heating and viscous dissipation on magnetohydrodynamic boundary layer flow of Jeffrey nanofluid over a vertically stretching cylinder. Coatings. 2021 Mar 19;11(3):353.
Available:https://doi.org/10.3390/coatings11030353

[5] Agbaje TM, Leach PG. Numerical Investigation of Natural Convection Viscoelastic Jeffrey's Nanofluid Flow from a Vertical Permeable Flat Plate with Heat Generation, Thermal Radiation, and Chemical Reaction. InAbstract and Applied Analysis 2020 Oct 20 (Vol. 2020). Hindawi.
Available:https://doi.org/10.1155/2020/9816942

[6] El-Zahar ER, Rashad AM, Seddek LF. Impacts of viscous dissipation and brownian motion on Jeffrey nanofluid flow over an unsteady stretching surface with thermophoresis. Symmetry. 2020 Sep 3;12(9):1450.
Available:https://doi.org/10.3390/sym12091450

[7] Ur Rasheed H, AL-Zubaidi A, Islam S, Saleem S, Khan Z, Khan W. Effects of Joule heating and viscous dissipation on magnetohydrodynamic boundary layer flow of Jeffrey nanofluid over a vertically stretching cylinder. Coatings. 2021 Mar 19;11(3):353.
Available:https://doi.org/10.3390/coatings11030353

[8] Ge-JiLe H, Qayyum S, Shah F, Khan MI, Khan SU. Slip flow of Jeffrey nanofluid with activation energy and entropy generation applications. Advances in Mechanical Engineering. 2021 Mar;13(3):16878140211006578.
Available:https://doi.org/10.1177/16878140211006578

[9] Ge-JiLe H, Qayyum S, Shah F, Khan MI, Khan SU. Slip flow of Jeffrey nanofluid with activation energy and entropy generation applications. Advances in Mechanical Engineering. 2021 Mar;13(3):16878140211006578.
Available:https://doi.org/10.1186/s13662-019-2222-1

[10] Srinivasacharya D, Shafeeurrahaman M. Mixed convection flow of nanofluid in a vertical channel with hall and ion-slip effects. Frontiers in Heat and Mass Transfer. 2017;8(5):950–959.
Available:https://doi.org/10.5098/hmt.8.11

[11] Hayat T, Qayyum S, Alsaedi A. Mechanisms of nonlinear convective flow of Jeffrey nanofluid due to nonlinear radially stretching sheet with convective conditions and magnetic field. Results in physics. 2017 Jan 1;7:2341-51.
Available:https://doi.org/10.1016/j.rinp.2017.06.052

[12] Shahzad F, Sagheer M, Hussain S. Numerical simulation of magnetohydrodynamic Jeffrey nanofluid flow and heat transfer over a stretching sheet considering Joule heating and viscous dissipation. AIP Advances. 2018 Jun 20;8(6):065316.
Available:https://doi.org/10.1063/1.5031447

[13] Saleem S, Rafiq H, Al-Qahtani A, El-Aziz MA, Malik MY, Animasaun IL. Magneto Jeffrey nanofluid bioconvection over a rotating vertical cone due to gyrotactic microorganism. Mathematical Problems in Engineering. 2019 May 12;2019.
Available:https://doi.org/10.1155/2019/3478037

[14] Rasool G, Shafiq A, Durur H. Darcy-Forchheimer relation in Magnetohydrodynamic Jeffrey nanofluid flow over stretching surface. Discrete & Continuous Dynamical Systems-S. 2021;14(7):2497.
Available:https://doi.org/10.3934/dcdss.2020399

Peer-review history:
The peer review history for this paper can be accessed here (Please copy paste the total link in your browser address bar)
https://www.sdiarticle5.com/review-history/88596